

## 两个镧系金属配合物的水热合成、晶体结构、 荧光、热稳定性及抑菌活性

宗广才<sup>1,2</sup> 任 宁<sup>\*3</sup> 张建军<sup>\*,1,2</sup> 祁晓霞<sup>1,2</sup> 高 捷<sup>1,2</sup> 张大海<sup>3</sup>

(<sup>1</sup> 河北师范大学, 分析测试中心, 石家庄 050024)

(<sup>2</sup> 河北师范大学, 化学与材料科学学院, 石家庄 050024)

(<sup>3</sup> 邯郸学院, 化学化工与材料学院, 邯郸 056005)

**摘要:** 水热法合成了 2 个镧系配合物  $[\text{Ln}(3,4\text{-DFBA})_3(\text{phen})(\text{H}_2\text{O})_2](\text{H}_2\text{O})_2$  ( $\text{Ln}=\text{Sm}$  (**1**),  $\text{Ho}$  (**2**); 3,4-DFBA=3,4-二氟苯甲酸根, phen=菲咯啉)。利用 X-射线单晶衍射仪测定了配合物的晶体结构。配合物 **1** 和 **2** 结构相同, 配位数为 8, 属于三斜晶系, 空间群为  $P\bar{1}$ 。相邻的 2 个双核分子之间通过分子间相互作用力形成了 2D 层状结构。并用元素分析, 红外, 紫外, XRD 等手段对目标配合物进行了表征。用 TG-DTG 技术测定了配合物的热稳定性, 同时对配合物 **1** 的荧光性能进行了研究。另外, 还测定了这两种配合物对白色念珠菌, 革兰氏阴性菌(大肠杆菌)以及革兰氏阳性菌(金黄色葡萄球菌)的抑菌活性。

**关键词:** 镧系元素; 3,4-二氟苯甲酸; 热分析; 荧光; 抑菌活性; 晶体结构

中图分类号: O614.33\*7; O614.343

文献标识码: A

文章编号: 1001-4861(2015)07-1425-08

DOI: 10.11862/CJIC.2015.176

## Hydrothermal Syntheses, Crystal Structures, Luminescence, Thermal Stabilities and Bacteriostatic Activities of Two Lanthanide Complexes

ZONG Guang-Cai<sup>1,2</sup> REN Ning<sup>\*3</sup> ZHANG Jian-Jun<sup>\*,1,2</sup> QI Xiao-Xia<sup>1,2</sup> GAO Jie<sup>1,2</sup> ZHANG Da-Hai<sup>3</sup>

(<sup>1</sup> Testing and Analysis Center, Hebei Normal University, Shijiazhuang 050024, China)

(<sup>2</sup> College of Chemistry & Material Science, Hebei Normal University, Shijiazhuang 050024, China)

(<sup>3</sup> College of Chemical Engineering & Material, Handan College, Handan, Hebei 056005, China)

**Abstract:** Two lanthanide complexes  $[\text{Ln}(3,4\text{-DFBA})_3(\text{phen})(\text{H}_2\text{O})_2](\text{H}_2\text{O})_2$  ( $\text{Ln}=\text{Sm}$  (**1**),  $\text{Ho}$  (**2**); 3,4-DFBA=3,4-difluorobenzoate, phen=1,10-phenanthroline) were prepared by hydrothermal method. Their structures were determined by single-crystal X-ray diffraction method. The structures of complexes **1** and **2** are isostructural with the coordination number of eight. They crystallized in the triclinic space group  $P\bar{1}$ . The 2D layered structure is formed by intermolecular forces of adjacent two binuclear molecules. The title complexes were characterized by elemental analysis, IR, UV, XRD, and so on. The thermal stability of the complexes was tested using TG-DTG technology. The luminescent property of complex **1** had been explored. Besides, the bacteriostatic activities of the two complexes to *candida albicans*, Gram negative bacteria (*escherichia coli*) and Gram positive bacteria (*staphylococcus aureus*) were also studied. CCDC: 1023982, **1**; 1023981, **2**.

**Key words:** lanthanides; 3,4-difluorobenzoic acid; thermal analysis; luminescence; bacteriostatic activity; crystal structure

收稿日期: 2015-03-13。收修改稿日期: 2015-04-20。

国家自然科学基金(No.21073053、21473049), 河北省自然科学基金(No.B2012205022)资助项目。

\*通讯联系人。E-mail: ningren9@163.com, jjzhang6@126.com; 会员登记号: S06N6096M1306(任宁), S06N9443M1404(张建军)。

The lanthanide coordination chemistry has become of increasing significance in the last few years<sup>[1]</sup>. Due to the larger radius of lanthanide ions and higher affinity for hard donor centers, lanthanide ions are easily to construct coordination polymers with organic carboxylic acid ligands and neutral ligands using regular methods<sup>[2]</sup>. Lanthanide complexes with fancy chemical and physical characters have potential applications as fluorescence materials and bioprobes and so on<sup>[3]</sup>. Since a lanthanide organic complex of europium emitted brightly photoluminescence was reported firstly by Weissman<sup>[4]</sup>, the fluorescence materials began to be studied and other lanthanide complexes with metal ions Sm(III), Tb(III), Dy(III) had been involved<sup>[5-7]</sup>. In addition, lanthanide complexes have high sterilization ability and wide inhibition zone, hence, the bacteriostatic activity of complexes is a popular topic over the years in the field of biological and other aspects<sup>[8-11]</sup>.

In this paper, two complexes  $[\text{Ln}(\text{3,4-DFBA})_3(\text{phen})(\text{H}_2\text{O})_2](\text{H}_2\text{O})_2$  ( $\text{Ln}=\text{Sm}$  (**1**),  $\text{Ho}$  (**2**); 3,4-DFBA=3,4-difluorobenzoate, phen =1,10-phenanthroline) have been synthesized by hydrothermal method. Complexes **1** and **2** are binuclear molecules. Two of  $\text{H}_2\text{O}$  molecules are coordinated with two metal ions and another two  $\text{H}_2\text{O}$  molecules are crystal water, which are rare in the study of lanthanide carboxylic acid complexes<sup>[12-14]</sup>. Thermal and luminescent properties, bacteriostatic activities of the title complexes are also investigated.

## 1 Experimental

### 1.1 Materials and measurement

All reagents and solvents were purchased commercially without further purification.  $\text{LnCl}_3 \cdot 6\text{H}_2\text{O}$  were prepared by the reaction of  $\text{Ln}_2\text{O}_3$  and hydrochloric acid in aqueous solution, followed by recrystallization and drying. The obtained complexes were dissolved in DMSO solution with the concentration of  $10 \mu\text{mol} \cdot \text{L}^{-1}$  and  $1 \text{ mmol} \cdot \text{L}^{-1}$  for the determination of ultraviolet spectra and molar conductivity, respectively. The contents of C, H and N were recorded on FLASH EA 1112 element analyzer (Thermo Fisher). The infrared spectrum were studied

with KBr discs technique by using the Bruker TENSOR 27 spectrometer at room temperature over the range of 4 000 to  $400 \text{ cm}^{-1}$ . Ultraviolet spectra were carried out on a U-3010 Spectrophotometer. The molar conductivity was measured by DDS-307 conductometer (Shanghai Precision & Scientific Instrument CO.LTD) at room temperature. X-ray Diffractions for complexes were tested on X-ray powder (Bruker AXS) diffractometer (Germany, D8 ADVANCE) with a scan speed of  $0.1^\circ \cdot \text{s}^{-1}$ ,  $\text{Cu K}\alpha$  radiation ( $\lambda=0.15418 \text{ nm}$ ), scan range from  $5^\circ$  to  $50^\circ$ . The thermal stability was investigated by TG/DTG using the NETZSCH STA 449 F3 with a heating rate of  $10 \text{ K} \cdot \text{min}^{-1}$  (Simulated air atmosphere). The fluorescent spectrum of complex **1** was depicted in an F-4500 Hitachi spectrophotometer at room temperature. The bacteriostatic activities were investigated by the disk diffusion method using the Mueller-Hinton agar medium. The bacteriostatic effects for *escherichia coli* and *staphylococcus aureus* were investigated at the temperature of 310 K, while *candida albicans* at 303 K.

### 1.2 Synthesis of the complexes

3,4-difluorobenzoic acid (3,4-DFHBA, 0.3 mmol) and 1,10-phenanthroline (0.1 mmol) were together dissolved in ethanol solution (95%) and the pH value of the solution was adjusted to 5~7 by adding  $1 \text{ mol} \cdot \text{L}^{-1}$  NaOH solution.  $\text{LnCl}_3 \cdot 6\text{H}_2\text{O}$  ( $\text{Ln}=\text{Sm}$  (**1**),  $\text{Ho}$  (**2**)) (0.1 mmol) was dissolved in distilled water. The resulting solution of the ligands was then added dropwise into the aqueous solution of lanthanide metal salts under stirring for 40 min. Subsequently, the mixture solution was transferred to the Teflon-lined autoclave and settled in electrothermal constant-temperature dry box at  $120^\circ \text{C}$  for 72 h<sup>[15-16]</sup>. Then the transparent crystals suitable for X-ray diffraction analysis were produced. Anal. Calcd. for  $\text{C}_{66}\text{H}_{42}\text{F}_{12}\text{N}_4\text{Sm}_2\text{O}_{16}$ (%): C, 47.31; H, 2.53; N, 3.34. Found(%): C, 47.70; H, 2.12; N, 3.33. Anal. Calcd. for  $\text{C}_{66}\text{H}_{42}\text{F}_{12}\text{N}_4\text{Ho}_2\text{O}_{16}$ (%): C, 46.50; H, 2.48; N, 3.29. Found(%): C, 46.74; H, 2.35; N, 3.29.

### 1.3 X-ray crystallography

A suitable crystal of complex **1** with dimensions of  $0.40 \text{ mm} \times 0.11 \text{ mm} \times 0.06 \text{ mm}$  was mounted on a

Smart-1000 (Bruker AXS) diffractometer with monochromated Mo  $K\alpha$  radiation ( $\lambda=0.071\ 073\ \text{nm}$ ) at 298 K. A total of 8 023 reflections were collected in the range of  $2.65^\circ \leq \theta \leq 25.02^\circ$  ( $-7 \leq h \leq 9$ ,  $-16 \leq k \leq 16$ ,  $-17 \leq l \leq 17$ ), and 5 452 reflections were independent with  $R_{\text{int}}=0.054\ 9$ , of which 4 297 reflections were observed with  $I > 2\sigma(I)$ .

A suitable crystal of complex **2** with dimensions of  $0.40\ \text{mm} \times 0.36\ \text{mm} \times 0.18\ \text{mm}$  was mounted on the diffractometer mentioned above. A total of 7 858

reflections were collected in the range of  $2.65^\circ \leq \theta \leq 25.02^\circ$  ( $-9 \leq h \leq 7$ ,  $-15 \leq k \leq 16$ ,  $-17 \leq l \leq 17$ ), and 5 316 reflections were independent with  $R_{\text{int}}=0.054\ 9$ , of which 4 497 reflections were observed with  $I > 2\sigma(I)$ .

The structures were solved by direct methods using the SHELXS-97 program and refined by full-matrix least-squares on  $F^2$  using the SHELXL-97 program<sup>[15]</sup>. The crystal data and structural refinement parameters of the complexes are listed in Table 1.

CCDC: 1023982, **1**; 1023981, **2**.

**Table 1** Crystal data and structural refinement parameters for complexes **1** and **2**

| Complex   | <b>1</b>  | <b>2</b>  |
|---|---|---|
| Empirical formula   | $\text{C}_{66}\text{H}_{42}\text{F}_{12}\text{N}_4\text{O}_{16}\text{Sm}_2$ | $\text{C}_{66}\text{H}_{42}\text{F}_{12}\text{N}_4\text{O}_{16}\text{Ho}_2$ |
| Formula weight  | 1 675.74  | 1 704.9   |
| Crystal system  | Triclinic   | Triclinic   |
| Space group   | $P\bar{1}$  | $P\bar{1}$  |
| $a / \text{nm}$   | 0.829 20(6)   | 0.807 25(6)   |
| $b / \text{nm}$   | 1.391 19(12)  | 1.412 62(13)  |
| $c / \text{nm}$   | 1.471 61(13)  | 1.456 90(12)  |
| $\alpha / (^\circ)$   | 105.582(2)  | 105.566(2)  |
| $\beta / (^\circ)$  | 98.025 0(10)  | 98.505 0(10)  |
| $\gamma / (^\circ)$   | 101.217(2)  | 101.567(2)  |
| $V / \text{nm}^3$   | 1.570 6(2)  | 1.531 7(2)  |
| $Z$   | 1   | 1   |
| $D_c / (\text{Mg} \cdot \text{m}^{-3})$                           | 1.772   | 1.848   |
| $\mu / \text{mm}^{-1}$  | 1.961   | 2.677   |
| $F(000)$  | 826   | 836   |
| Completeness to $\theta=25.02^\circ / \%$                         | 98.30   | 98.40   |
| Max. and min. transmission  | 0.891 4 and 0.507 6   | 0.644 4 and 0.414 0   |
| Data / restraints / parameters                                    | 5 452 / 2 / 461   | 5 316 / 0 / 461   |
| Goodness-of-fit on $F^2$  | 1.077   | 0.995   |
| Final $R$ indices ( $I > 2\sigma(I)$ )                            | $R_1=0.052\ 3$ , $wR_2=0.106\ 5$  | $R_1=0.038\ 6$ , $wR_2=0.091\ 6$  |
| $R$ indices (all data)  | $R_1=0.067\ 0$ , $wR_2=0.111\ 3$  | $R_1=0.048\ 1$ , $wR_2=0.096\ 4$  |
| Largest diff. peak and hole / ( $\text{e} \cdot \text{nm}^{-3}$ ) | 1 302 and $-1\ 374$   | 1 736 and $-1\ 160$   |

## 2 Results and discussion

### 2.1 Infrared spectra

The infrared spectra of the complexes and the ligands are displayed in Table S1. The carboxylic acid ligand exhibits an intense C=O stretching vibration band at  $1\ 694\ \text{cm}^{-1}$ . While the  $\nu_{\text{C=O}}$  disappears in the IR spectrum of complexes **1** and **2**. The two absorbing bands assigned to the asymmetric ( $\nu_{\text{as}(\text{COO}_2)}$ ) and

symmetric ( $\nu_{\text{s}(\text{COO}_2)}$ ) vibrations are observed at  $1\ 544 \sim 1\ 547\ \text{cm}^{-1}$  and  $1\ 431\ \text{cm}^{-1}$ , respectively. Besides, the apparent band at  $419\ \text{cm}^{-1}$  is attributed to the  $\nu_{(\text{Ln-O})}$  of the two complexes. These all indicate that the oxygen atoms of 3,4-DFBA ligand takes part in coordination to the Ln(III) ion<sup>[18]</sup>. As shown in Table S1, the  $\nu_{\text{C=N}}$  and  $\delta_{\text{C-H}}$  bands in the IR spectra of complexes show a shift to a low frequency as compared with the free 1,10-phenanthroline ligand, indicating that two nitrogen

atoms of the ligand are coordinated to the Ln(III) ion<sup>[19]</sup>.

## 2.2 Ultraviolet spectra

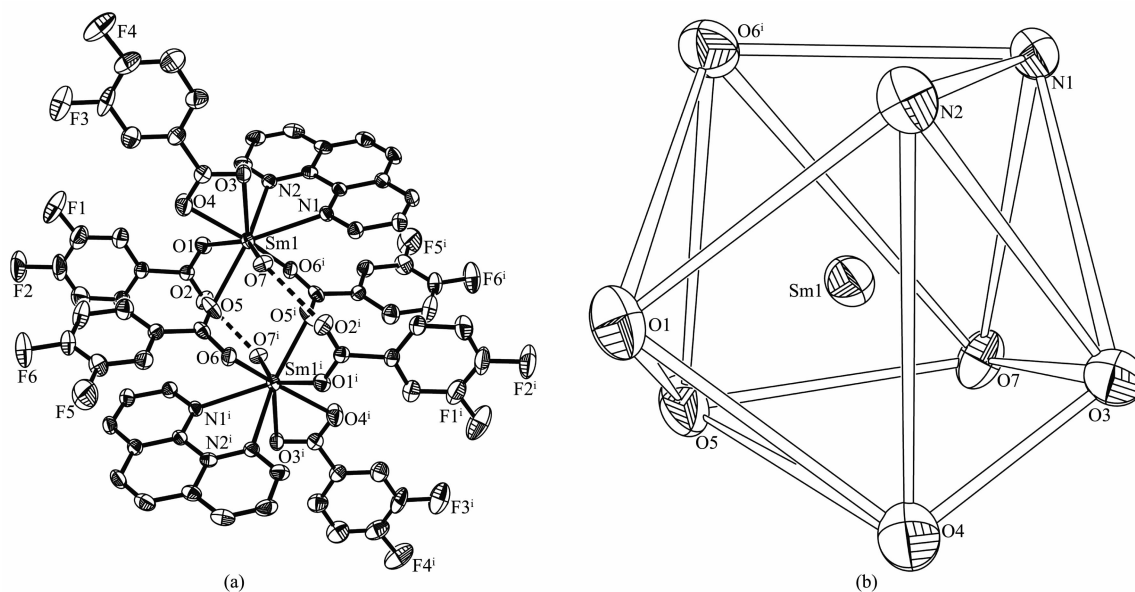
UV spectra of the two ligands and the title complexes are recorded in DMSO solution with DMSO as a reference. The data of UV absorption of the ligands and complexes are listed in Table S2. The intense band (255 nm) of 3,4-DFHBA ligand shifts to 265 nm in complexes. This may be explained by the expansion of the  $\pi$ -conjugated system due to metal coordination<sup>[20]</sup>. The maximum absorption wavelength ( $\lambda_{\max}$ ) of 1,10-phenanthroline is similar to that in the complexes, suggesting that the formation of Ln-N has no remarkable influence on ultraviolet absorption of 1,10-phenanthroline. The values of  $A_{\max}$  for complexes **1** and **2** are stronger than that of two ligands. It can be concluded that a larger chelate ring is constructed after coordination to the Ln(III) ions<sup>[21]</sup>.

## 2.3 Crystal structures

The molecular structures of complexes **1** and **2** with the coordination geometry of the Sm(III) and Ho(III) ions are shown in Fig.1 and Fig.S1. The selected bond lengths of complexes **1** and **2** are listed in Table 2. Because the crystal structures of the two complexes are isostructural, hence complex **1** is taken as an example to discuss in detail. As shown in Fig.1,

complex **1** is binuclear and crystallizes in the triclinic  $P\bar{1}$  space. Each Sm(III) ion is eight-coordinated by six O atoms and two N atoms, which resembles a distorted square antiprism geometry. These eight atoms are in three models of bidentate bridging (O5, O6<sup>i</sup>), bidentate chelating (O3, O4 and N1, N2) and monodentate (O1, O7) to coordinate with the center Sm(III) ion. Besides, another two water molecules are not involved in coordination with Sm(III) but exist freely in the binuclear crystal structure. It is worth noting that intramolecular hydrogen bond is formed between O7<sup>i</sup> and O2, O7 and O2<sup>i</sup>. Further more, the adjacent two binuclear molecules form two-dimensional layered structure by intermolecular forces for complex **1**, as shown in Fig.2. The hydrogen bond distances in complexes **1** and **2** are given in Table S3.

The average distance of Sm(1)-O is 0.243 2(3) nm and that of Ho(1)-O is 0.234 3(7) nm. The average distance of Sm(1)-N and Ho(1)-N are 0.260 7(0) nm and 0.253 2(5) nm, respectively. The length of Ln-O is always shorter than that of Ln-N, which proves the stronger combination ability of Ln to O than N<sup>[22]</sup>. The result can explain why 1,10-phenanthroline ligand is lost firstly in the decomposition process.

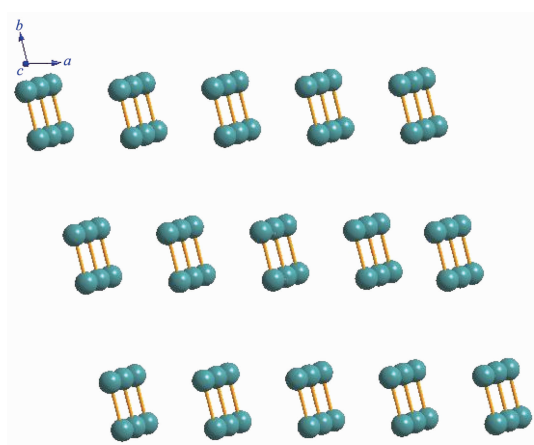


All hydrogen atoms are omitted for clarity and thermal ellipsoids are drawn at the 30% probability level; Symmetry code: <sup>i</sup>  $-x+1, -y+1, -z+1$ ; The intramolecular hydrogen bond is displayed by a dotted line

Fig.1 (a) Molecular structure of complex **1**; (b) Coordination geometry of the Sm(III) ion

**Table 2** Selected bond lengths of the complexes **1** and **2**

| 1                       |            | 2                       |            |
|-------------------------|------------|-------------------------|------------|
| Sm(1)-O(1)              | 0.234 6(4) | Ho(1)-O(1)              | 0.228 2(4) |
| Sm(1)-O(7)              | 0.241 2(4) | Ho(1)-O(6) <sup>i</sup> | 0.230 0(4) |
| Sm(1)-O(5)              | 0.243 4(5) | Ho(1)-O(5)              | 0.230 7(4) |
| Sm(1)-O(4)              | 0.243 6(5) | Ho(1)-O(7)              | 0.233 5(4) |
| Sm(1)-O(6) <sup>i</sup> | 0.244 0(5) | Ho(1)-O(4)              | 0.236 4(4) |
| Sm(1)-O(3)              | 0.252 3(4) | Ho(1)-O(3)              | 0.247 2(4) |
| Average length of Ln-O  | 0.243 2(3) |                         | 0.234 3(7) |
| Sm(1)-N(2)              | 0.257 0(5) | Ho(1)-N(2)              | 0.249 9(4) |
| Sm(1)-N(1)              | 0.264 3(5) | Ho(1)-N(1)              | 0.256 5(5) |
| Average length of Ln-N  | 0.260 7(0) |                         | 0.253 2(5) |



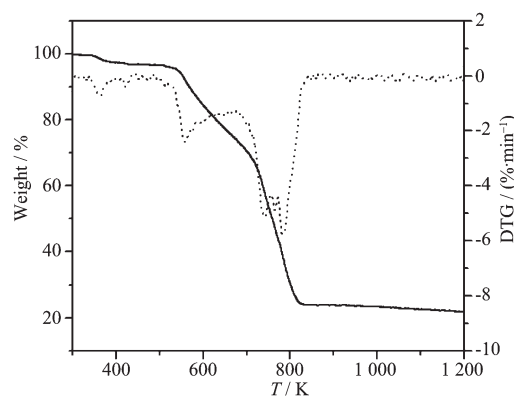
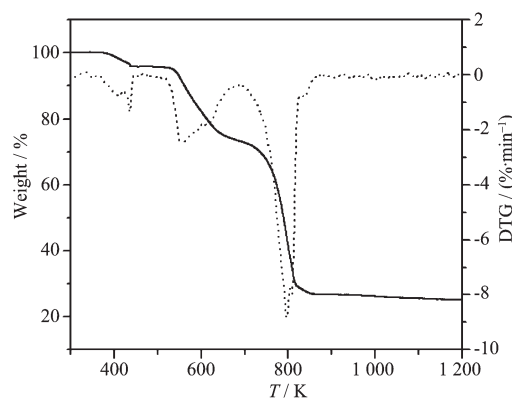
All atoms except samarium are omitted for clarity

**Fig.2** A two-dimensional layered structure of complex **1**

## 2.4 Thermal analysis

TG-DTG curves of the title complexes are shown in Fig.3 and 4. For complex **1**, the decomposition process can be divided into three steps. The first step begins at 338.15 K and ends at 441.15 K with a weight loss of 2.48%, assigning to the loss of two crystallization water molecules (Calcd. 2.15%). The second degradation stage is in the range of 441.15~659.15 K with weight loss of 22.94%, corresponding to the loss of another two coordinated water molecules and two 1,10-phenanthroline molecules (Calcd. 23.67%). The third weight loss of 52.83% between 676.15 K and 1 363.45 K is attributed to the loss of all 3,4-DFBA ligands. In summary, the total loss rate is 78.25% with a theoretical value of 79.20% if Sm<sub>2</sub>O<sub>3</sub> was the final products. For complex **2** (Fig.4), to begin with, all water molecules are released from 344.15 K to 459.15 K (Found 4.29%, Calcd. 4.22%). The

following decomposition belongs to the loss of 1,10-phenanthroline molecules with a value of 21.76% (Calcd. 21.14%). To the end, the complex **2** is completely degraded into Ho<sub>2</sub>O<sub>3</sub>.

**Fig.3** TG-DTG curves of complex **1****Fig.4** TG-DTG curves of complex **2**

## 2.5 Powder X-ray diffraction

The PXRD patterns of the title complexes were checked at room temperature, as shown in Fig.S2. The peak positions of the simulated and experimental PXRD patterns are in agreement with each other,

which demonstrate the good phase purity of the complexes.

## 2.6 Fluorescence spectrum

Because of the orange-red emission of Sm(III) ion, the complex **1** has been demonstrated to be potential application in full-color fluorescence materials for applications as full-color fluorescence materials. The emission spectrum of complex **1** under excitation at 335 nm is displayed in Fig.5. The characteristic fluorescence of Sm(III) ion (at 601 nm) corresponding to the  $^4G_{5/2} \rightarrow ^6F_{7/2}$  are detected<sup>[23]</sup>, and another two emission

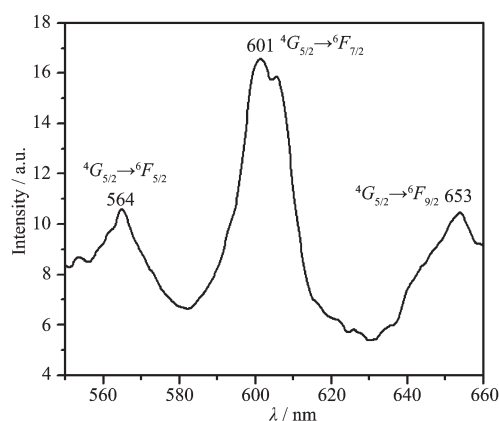


Fig.5 Solid state emission spectra of complex **1**  
( $\lambda_{ex}$ =335 nm)

peaks at 564 nm and 653 nm are attributed to the transitions of  $^4G_{5/2} \rightarrow ^6F_{5/2}$ ,  $^4G_{5/2} \rightarrow ^6F_{9/2}$ , respectively.

## 2.7 Bacteriostatic activity

The bacteriostatic circles diameter of the complexes **1** and **2** with different concentrations to *escherichia coli*, *staphylococcus aureus* and *candida albicans* are shown in Table 3~5. The temperature of 310 K is optimum for bacteria (*escherichia coli*, *staphylococcus aureus*) growth. While 303 K is optimum for fungus (*candida albicans*) growth. As can be seen from Table 3 and 4, the bacteriostatic circles diameter is 6 mm with the concentration of 8 mmol·L<sup>-1</sup>. Then with the increase of solution concentration, the bacteriostatic circles diameter increases. In other words, the concentration of the complex is higher, the bacteriostatic effect is more obvious.

As shown in Table 5, with a concentration of 8 mmol·L<sup>-1</sup>, average diameter bacteriostatic circles for complexes **1** and **2** are 11.10 and 13.37 mm, respectively, which is larger than 6 mm of filter diameter itself. This confirms that complexes have remarkable bacteriostatic action to *candida albicans* even at low concentration. Besides, bacteriostatic actions are more

Table 3 Bacteriostatic activities of complexes **1** and **2** to *escherichia coli* (T=310 K)

| Complexes | Concentration / (mmol·L <sup>-1</sup> ) | Diameter of bacteriostatic circles* / mm |       |       |         |
|-----------|---|--|-------|-------|---------|
|           |   | ①  | ②     | ③     | Average |
| <b>1</b>  | 8                                       | 6.00                                     | 6.00  | 6.00  | 6.00    |
|           | 16                                      | 8.70                                     | 9.00  | 8.30  | 8.67    |
|           | 32                                      | 12.90                                    | 14.50 | 12.50 | 13.30   |
| <b>2</b>  | 8                                       | 6.00                                     | 6.00  | 6.00  | 6.00    |
|           | 16                                      | 8.70                                     | 8.80  | 8.50  | 8.67    |
|           | 32                                      | 15.60                                    | 14.50 | 15.90 | 15.33   |

\*Three times in parallel; the filter diameter is 6 mm.

Table 4 Bacteriostatic activities of complexes **1** and **2** to *staphylococcus aureus* (T=310 K)

| Complexes | Concentration / (mmol·L <sup>-1</sup> ) | Diameter of bacteriostatic circles* / mm |       |       |         |
|-----------|---|--|-------|-------|---------|
|           |   | ①  | ②     | ③     | Average |
| <b>1</b>  | 8                                       | 6.00                                     | 6.00  | 6.00  | 6.00    |
|           | 16                                      | 8.30                                     | 8.30  | 8.40  | 8.33    |
|           | 32                                      | 12.40                                    | 12.10 | 13.70 | 12.73   |
| <b>2</b>  | 8                                       | 6.00                                     | 6.00  | 6.00  | 6.00    |
|           | 16                                      | 9.00                                     | 8.70  | 8.90  | 8.87    |
|           | 32                                      | 14.80                                    | 13.70 | 14.60 | 14.37   |

\*Three times in parallel; the filter diameter is 6 mm.



Table 5 Bacteriostatic activities of complexes **1** and **2** to *candida albicans* ( $T=303\text{ K}$ )

| Complexes | Concentration / (mmol·L <sup>-1</sup> ) | Diameter of bacteriostatic circles* / mm |       |       |         |
|-----------|---|--|-------|-------|---------|
|           |   | ①  | ②     | ③     | Average |
| <b>1</b>  | 8                                       | 11.60                                    | 11.50 | 10.20 | 11.10   |
|           | 16                                      | 17.50                                    | 17.30 | 16.70 | 17.17   |
|           | 32                                      | 21.60                                    | 21.00 | 22.10 | 21.57   |
| <b>2</b>  | 8                                       | 12.30                                    | 14.10 | 13.70 | 13.37   |
|           | 16                                      | 18.70                                    | 17.20 | 17.00 | 17.63   |
|           | 32                                      | 23.60                                    | 25.00 | 23.80 | 24.13   |

\*Three times in parallel; the filter diameter is 6 mm.

and more obvious with the increase of concentration, which is similar with *escherichia coli* and *staphylococcus aureus*.

Lanthanide complexes has certain bacteriostatic actions against microorganism, and it is generally recognized that Ln(III) ions are coordinated with the donor atoms of the ligands. This leads to the  $\pi$ -electron delocalization over the chelate ring further to reduces the polarity of the central metal ion. All phenomenon in turn favors permeation to the lipid layer of the membrane for lanthanide complexes<sup>[24-26]</sup>.

### 3 Conclusions

In summary, two complexes [Sm(3,4-DFBA)<sub>3</sub>(phen)(H<sub>2</sub>O)]<sub>2</sub>(H<sub>2</sub>O)<sub>2</sub> (**1**) and [Ho(3,4-DFBA)<sub>3</sub>(phen)(H<sub>2</sub>O)]<sub>2</sub>(H<sub>2</sub>O)<sub>2</sub> (**2**) were synthesized and characterized. Both of them were binuclear and isostructural with the space group of  $P\bar{1}$ . The intramolecular hydrogen bond is formed in complexes **1** and **2**. Thermal decomposition processes of the two complexes were divided into three steps. The emission spectrum of complex **1** under excitation at 335 nm indicated the characteristic fluorescence of Sm(III) ion corresponding to the  $^4G_{5/2} \rightarrow ^6F_{7/2}$ . Bacteriostatic activities of these complexes to Gram bacteria bacteria (*escherichia coli*), Gram negative positive (*staphylococcus aureus*) and *candida albicans* have obvious effects at high concentration.

Supporting Information is available at <http://www.wjhxsb.cn>

### References:

- [1] Hasegawa Y, Wada Y, Yanagida S. *J. Photochem. Photobiol. C*, **2004**, *5*:183-202
- [2] Yang L R, Liu L, Wu L Z, et al. *Dyes Pigm.*, **2014**, *111*:176-184
- [3] Li W X, Guo F, Zheng Y S, et al. *J. Lumin.*, **2014**, *153*:421-429
- [4] Weissman S I. *J. Chem. Phys.*, **1942**, *10*:214-217
- [5] Ni Y R, Tao J, Jin J Y, et al. *J. Alloys Compd.*, **2014**, *612*:349-354
- [6] Li L F, Dong D B, Zhang J Y, et al. *Mater. Lett.*, **2014**, *131*:298-301
- [7] Li W X, Feng S Y, Liu Y, et al. *J. Lumin.*, **2013**, *143*:746-753
- [8] Lekha L, Raja K K, Rajagopal G, et al. *J. Mol. Struct.*, **2014**, *1056-1057*:307-313
- [9] Kulkarni A, Patil S A, Badami P S. *Eur. J. Med. Chem.*, **2009**, *44*:2904-2912
- [10] Subhan M A, Rahman M S, Alam K, et al. *Spectrochim. Acta A*, **2014**, *118*:944-950
- [11] Lima L M P, Delgado R, Marques F, et al. *Eur. J. Med. Chem.*, **2010**, *45*:5621-5627
- [12] Li X, Zhang Z Y, Zou Y Q. *Eur. J. Inorg. Chem.*, **2005**, *14*:2909-2918
- [13] Li Y, Zheng F K, Liu X, et al. *Inorg. Chem.*, **2006**, *45*:6308-6316
- [14] Ma D, Li X, Huo R. *J. Mater. Chem. C*, **2014**, *43*:9073-9076
- [15] Wang J F, Li H, Zhang J J, et al. *Sci. China Ser. B Chem.*, **2012**, *55*:2161-2175
- [16] Yang Z H, Xu J, Zhang W X, et al. *J. Solid State Chem.*, **2007**, *180*:1390-1396
- [17] Sheldrick G M. *SHELXTL-97, Programs for Crystal Structure Refinement*, University of Göttingen, Germany, **1997**.
- [18] Zhou X J, Zhao X Q, Wang Y J, et al. *Inorg. Chem.*, **2014**, *53*:12275-12282
- [19] Zheng J R, Ren N, Zhang J J, et al. *J. Chem. Thermodyn.*, **2013**, *57*:169-177
- [20] An B L, Gong M L, Li M X, et al. *J. Mol. Struct.*, **2004**, *687*:1-6
- [21] ZHANG Ying-Ying (张莹莹), REN Shu-Xia (任书霞),

- ZHANG Jian-Jun(张建军), et al. *Chinese Sci. Bull.*(科学通报), **2014**,**59**(27):3398-3405
- [22]Łyszczyk R, Rzaczyńska Z, Kula A, et al. *J. Anal. Appl. Pyrolysis*, **2011**,**92**:347-354
- [23]Liu D, Yu H, Wang Z G, et al. *Polym. Int.*, **2010**,**59**:937-94
- [24]Hang J, Xu Y H, Chen X K, et al. *J. Rare Earths*, **2012**,**30**:586-591
- [25]Liu J Y, Ren N, Zhang J J, et al. *Thermochim. Acta*, **2013**,**570**:51-58
- [26]Zhao Y F, Chu H B, Bai F, et al. *J. Organomet. Chem.*, **2012**,**716**:167-174